Electronic Supplementary Material (ESI) for Journal of Materials Chemistry A.
This journal is © The Royal Society of Chemistry 2019

Electronic Supplementary Information (ESI)

A Ca^{2+} MOF combining highly efficient sorption and capability for voltammetric determination of heavy metal ions in aqueous media

Anastasia D. Pournara,[a] Antigoni Margariti,[b] Georgios D. Tarlas,[b] Andreas Kourtelaris,[c] Valeri Petkov,[d] Christos Kokkinos,[e] Anastasios Economou,[e] Giannis S. Papaefstathiou *[b] and Manolis J. Manos *[a]

[a.] *Laboratory of Inorganic Chemistry, Department of Chemistry, University of Ioannina, 45110 Ioannina, Greece. E-mail: emanos@cc.uoi.gr*

[b.] *Laboratory of Inorganic Chemistry, Department of Chemistry, National and Kapodistrian University of Athens, Panepistimiopolis, 157 71, Zografou, Greece. E-mail: gspapaef@chem.uoa.gr*

[c.] *Department of Chemistry, University of Cyprus, 1678 Nicosia, Cyprus.*

[d.] *Department of Physics and Science of Advanced Materials Program, Central Michigan University, Mt. Pleasant, Michigan 48859, USA.*

[e.] *Laboratory of Analytical Chemistry, Department of Chemistry, National and Kapodistrian University of Athens, Panepistimiopolis, 157 71, Zografou, Greece.*

Synthesis of $[Ca(H_4L)(DMA)_2]\cdot 2DMA$ (Ca-MOF)

Solid H_6L (25 mg, 0.06 mmol) and solid $Ca(NO_3)_2\cdot 4H_2O$ (14 mg, 0.06 mmol) were added in a 24 mL glass vial containing DMA (5 ml). The mixture was stirred for 5 min to afford a white-yellowish non-clear solution. The glass vial was sealed and heated in an isotemp oven at 100 ˚C for 3 days. Colorless plate-like single-crystals of **Ca-MOF** were formed. Yield 34mg (~70 % based on Ca). The crystals were collected by vacuum filtration and dried in a desiccator over silica gel. Anal. Calcd for $C_{34}H_{46}N_6O_{14}Ca$: C 50.86 , H 5.78, N 10.46; found: C 50.74, H 5.67, N 10.51. IR (KBr pellets, cm^{-1}): 3419 wbr, 2934 w, 2448 wbr, 1684 s, 1660 s, 1624 vs, 1575 s, 1512 vs, 1443 s, 1423 s, 1370 w, 1299 m, 1263 m, 1165 w, 1026 m, 1012 m, 949 w, 912 w, 866 w, 805 m, 769 m, 758 m, 696 w, 678 w, 596 m, 570 m, 517 m, 485 m.

Table S1. Crystal data and structure refinement for complexes **1** and **2**.

Code	**1**[a]	**2**[b]
Empirical formula	C24 H20 N4 Ni O16	C9 H4 N O6 Pb
Formula weight	679.13	429.32
Temperature	100(2) K	293(2) K
Wavelength	1.54184 Å	1.54184 Å
Crystal system	monoclinic	orthorhombic
Space group	C2/c	Pbcn
Unit cell dimensions	a = 21.7280(9) Å, α = 90° b = 10.3246(4) Å, β = 98.983(4)° c = 13.1378(5) Å, γ = 90°	a = 4.1673(2) Å, α = 90° b = 25.707(2) Å, β = 90° c = 18.2223(9) Å, γ = 90°
Volume	2911.1(2) $Å^3$	1952.2(2) $Å^3$
Z	4	8
Density (calculated)	1.550 g/cm^3	2.922 g/cm^3
Absorption coefficient	1.716 mm^{-1}	33.853 mm^{-1}
F(000)	1392	1560
Crystal size	0.08 x 0.03 x 0.01 mm^3	0.02 x 0.01 x 0.01 mm^3
θ range for data collection	4.120 to 73.375°	4.209 to 66.964°
Index ranges	-26<=h<=26, -12<=k<=9, -15<=l<=16	-4<=h<=4, -29<=k<=30, -21<=l<=19
Reflections collected	8800	6617
Independent reflections	2891 [R_{int} = 0.0323]	1708 [R_{int} = 0.0603]
Completeness to θ = 67.684°	100%	98.7%
Refinement method	Full-matrix least-squares on F^2	Full-matrix least-squares on F^2
Data / restraints / parameters	2891 / 0 / 205	1708 / 75 / 157
Goodness-of-fit	1.064	1.142
Final R indices [I > 2σ(I)]	R_{obs} = 0.0479, wR_{obs} = 0.1426	R_{obs} = 0.0870, wR_{obs} = 0.2808
R indices [all data]	R_{all} = 0.0551, wR_{all} = 0.1508	R_{all} = 0.1134, wR_{all} = 0.3049
Largest diff. peak and hole	0.949 and -0.453 e·$Å^{-3}$	3.674 and -3.237 e·$Å^{-3}$
CCDC	1905925	1905924

[a] $R = \Sigma||F_o|-|F_c|| / \Sigma|F_o|$, $wR = \{\Sigma[w(|F_o|^2 - |F_c|^2)^2] / \Sigma[w(|F_o|^4)]\}^{1/2}$ and $w=1/[\sigma^2(Fo^2)+(0.0955P)^2+4.2718P]$ where $P=(Fo^2+2Fc^2)/3$

[b] $R = \Sigma||F_o|-|F_c|| / \Sigma|F_o|$, $wR = \{\Sigma[w(|F_o|^2 - |F_c|^2)^2] / \Sigma[w(|F_o|^4)]\}^{1/2}$ and $w=1/[\sigma^2(Fo^2)+(0.1820P)^2+12.2758P]$ where $P=(Fo^2+2Fc^2)/3$

Table S2. Selected interatomic distances (Å) and angles (°) for complexes **1** and **2**.

1		**2**	
Ni(1)-O(7)#1	2.0476(17)	Pb(2)-O(5)	2.399(13)
Ni(1)-O(7)	2.0476(17)	Pb(2)-O(5)#2	2.399(14)
Ni(1)-O(6)#1	2.0520(17)	Pb(2)-O(4)#3	2.500(14)
Ni(1)-O(6)	2.0521(17)	Pb(2)-O(4)#4	2.500(14)
Ni(1)-O(2)	2.0854(15)	Pb(1)-O(1)	2.35(2)
Ni(1)-O(2)#1	2.0854(15)	Pb(1)-O(1)#5	2.35(2)
O(7)#1-Ni(1)-O(7)	180.00(6)	Pb(1)-O(2)#6	2.67(2)
O(7)#1-Ni(1)-O(6)#1	88.14(7)	Pb(1)-O(2)#7	2.67(2)
O(7)-Ni(1)-O(6)#1	91.86(7)	Pb(1)-O(2)#5	2.72(2)
O(7)#1-Ni(1)-O(6)	91.86(7)	Pb(1)-O(2)	2.72(2)
O(7)-Ni(1)-O(6)	88.14(7)	O(5)-Pb(2)-O(5)#2	73.1(7)
O(6)#1-Ni(1)-O(6)	180.0	O(5)-Pb(2)-O(4)#3	78.2(5)
O(7)#1-Ni(1)-O(2)	94.19(7)	O(5)#1-Pb(2)-O(4)#3	86.8(5)
O(7)-Ni(1)-O(2)	85.81(7)	O(5)-Pb(2)-O(4)#4	86.8(5)
O(6)#1-Ni(1)-O(2)	87.74(6)	O(5)#1-Pb(2)-O(4)#4	78.2(5)
O(6)-Ni(1)-O(2)	92.26(6)	O(4)#2-Pb(2)-O(4)#4	161.3(8)
O(7)#1-Ni(1)-O(2)#1	85.81(7)	O(1)-Pb(1)-O(1)#5	77.0(10)
O(7)-Ni(1)-O(2)#1	94.19(7)	O(1)-Pb(1)-O(2)#6	80.2(8)
O(6)#1-Ni(1)-O(2)#1	92.26(6)	O(1)#4-Pb(1)-O(2)#6	96.1(8)
O(6)-Ni(1)-O(2)#1	87.74(6)	O(1)-Pb(1)-O(2)#7	96.1(8)
O(2)-Ni(1)-O(2)#1	180.0	O(1)#4-Pb(1)-O(2)#7	80.2(8)
		O(2)#5-Pb(1)-O(2)#7	175.4(8)
		O(1)-Pb(1)-O(2)#5	122.4(7)
		O(1)#4-Pb(1)-O(2)#5	53.3(7)
		O(2)#5-Pb(1)-O(2)#5	78.4(7)
		O(2)#6-Pb(1)-O(2)#5	101.4(7)
		O(1)-Pb(1)-O(2)	53.3(7)
		O(1)#4-Pb(1)-O(2)	122.4(7)
		O(2)#5-Pb(1)-O(2)	101.4(7)
		O(2)#6-Pb(1)-O(2)	78.4(7)
		O(2)#4-Pb(1)-O(2)	175.4(8)

Symmetry transformations used to generate equivalent atoms:

(1) -x+1,-y,-z+2 (2) -x,y,-z+3/2 (3) x-1,y,z (4) -x+1,y,-z+3/2 (5) -x+2,y,-z+1/2 (6) x+1,y,z (7) -x+1,y,-z+1/2

Table S3. Comparison of the metal ion (Pb^{2+}, Cd^{2+}, Ni^{2+}, Zn^{2+}) sorption capacities of **Ca-MOF** with those of other MOFs.

Target	*MOF-based sorbent*	*Capacity mg/g*	*Equilibrium time*	*Selectivity*	*Reusability*	*ref*
Pb^{2+}	MIL-53(Al) MFC	492.4	120min	-	-	R. Ricco, K. Konstas, M. J. Styles, J. J. Richardson, R. Babarao, K. Suzuki, P. Scopece and P. Falcaro, *J. Mater. Chem. A*, 2015, **3**, 19822–19831.
Pb^{2+}	TMU-5	251	5min	-	-	E. Tahmasebi, M. Y. Masoomi, Y. Yamini and A. Morsali, *Inorg. Chem.*, 2014, **54**, 425–433.
Pb^{2+}	Thiol-functionalized Fe_3O_4@$Cu_3(btc)_2$	215.05	120min	vs. various cations	reusable	F. Ke, J. Jiang, Y. Li, J. Liang, X. Wan and S. Ko, *Appl. Surf. Sci.*, 2017, **413**, 266–274.
Pb^{2+}	MCNC@Zn-BTC	558.66	30min	vs. Cu^{2+}, Zn^{2+}, Cd^{2+}	reusable	N. Wang, X. Ouyang, L. Yang and A. M. Omer, *ACS Sustainable Chem. Eng.*, 2017, **5**, 10447–10458
Pb^{2+}	$[Zn_3L_3(BPE)_{1.5}]_n$	616.64	10min	vs. Na^{+}, Mg^{2+}, K^{+}, Ca^{2+}, Mn^{2+}, Co^{2+}, Ni^{2+}, Cd^{2+}	Reusable	C. Yu, Z. Shao, and H. Hou, *Chem. Sci.*, 2017, **8**, 7611–7619.
Pb^{2+}	**Ca-MOF**	**522**	**5min**	**vs. Na^{+}, Mg^{2+}, Ca^{2+}, Ni^{2+}, Zn^{2+}, Cu^{2+}**	**recyclable**	**This work**
Cd^{2+}	NH_2-Zr-MOFs	177.35	120min	-	-	K. Wang, J. Gu and N. Yin, *Ind. Eng. Chem. Res.*, 2017, **56**, 1880–1887.
Cd^{2+}	FJI-H9	225	NA	vs. various cations	reusable	H. Xue, Q. Chen, F. Jiang, D. Yuan, G. Lv, L. Liang, L. Liu, and M. Hong, *Chem. Sci.*, 2016, **7**, 5983–5988.
Cd^{2+}	**Ca-MOF**	**220**	**2min**	**vs. Na^{+}, Mg^{2+}, Ca^{2+}, Ni^{2+}, Zn^{2+}, Cu^{2+}**	**recyclable**	**This work**
Ni^{2+}	**Ca-MOF**	**84**	**5min**	**vs. Na^{+}, Mg^{2+}, Ca^{2+}**	**recyclable**	**This work**
Zn^{2+}	**Ca-MOF**	**81**	**5min**	**vs. Na^{+}, Mg^{2+}, Ca^{2+}**	**recyclable**	**This work**

Table S4. Comparison of the metal ion (Pb^{2+}, Cd^{2+}, Ni^{2+}, Zn^{2+}) sorption capacities of **Ca-MOF** with those of other state-of-the-art sorbents (besides MOFs).

Target	*Sorbent*	*Capacity mg/g*	*Equilibrium time*	*Selectivity*	*Reusability*	*ref*
Pb^{2+}	KMS-1	377	5 min	vs. alkali and alkaline earth cations	Not reusable	M. J. Manos and M. G. Kanatzidis, *Chem.–Eur. J.*, 2009, **15**, 4779–4784
Pb^{2+}	Mg-MTMS	365	120 min	-	reusable	I. L. Lagadic, M. K. Mitchell, B. D. Payne, *Environ. Sci. Technol.*, 2001, **35**, 984 –990
Pb^{2+}	MoS_4-LDH	290	30 min	vs. Co^{2+}, Ni^{2+}, Zn^{2+}, Cd^{2+}	Not reusable	L. Ma, Q. Wang, S. M. Islam, Y. Liu, S. Ma and M. G. Kanatzidis, *J. Am. Chem. Soc.*, 2016, **138**, 2858–2866
Pb^{2+}	S_x -LDH	483	-	vs. Zn^{2+}, Co^{2+}, Ni^{2+}	Not reusable	S. Ma, Q. Chen, H. Li, P. Wang, S. M. Islam, Q. Gu, X. Yang and M. G. Kanatzidis, *J. Mater. Chem. A*, 2014, **2**, 10280–10289
Pb^{2+}	Duolite GT-73	238	-	-	-	S. Chamarthy, C. W. Seo, W. E. Marshall, *J. Chem. Technol. Biotechnol.*, 2001, **76**, 593 – 597.
Pb^{2+}	Amberlite IRC-718	477	-	-	-	S. Chamarthy, C. W. Seo, W. E. Marshall, *J. Chem. Technol. Biotechnol.*, 2001, **76**, 593 – 597.
Pb^{2+}	**Ca-MOF**	**522**	**5 min**	**vs. Na^+, Mg^{2+}, Ca^{2+}, Ni^{2+}, Zn^{2+}, Cu^{2+}**	**recyclable**	**This work**
Cd^{2+}	KMS-1	329	5 min	vs. alkali and alkaline earth cations	Not reusable	M. J. Manos and M. G. Kanatzidis, *Chem.–Eur. J.*, 2009, **15**, 4779–4784
Cd^{2+}	Mg-MTMS	210	-	-	-	H. Xue, Q. Chen, F. Jiang, D. Yuan, G. Lv, L. Liang, L. Liu, and M. Hong, *Chem. Sci.*, 2016, **7**, 5983–5988.
Cd^{2+}	SOL-AD-IV	222	-	vs. Ni^{2+}, Pb^{2+}, Zn^{2+}	-	J. S. Lee, S. Gomez-Salazar, L. L. Tavlarides, *React. Funct. Polym.*, 2001, **49**, 159 –172.
Cd^{2+}	Amberlite IRC-718	202	-	-	-	S. Chamarthy, C. W. Seo, W. E. Marshall, *J. Chem. Technol. Biotechnol.*, 2001, **76**, 593 – 597.
Cd^{2+}	KTS-3	209	5 min	vs. alkali and alkaline earth cations	Not reusable	D. Sarma, S. M. Islam, K. S. Subrahmanyam and M. G. Kanatzidis, ***J. Mater. Chem. A***, 2016, **4**, 16597-16605
Cd^{2+}	**Ca-MOF**	**220**	**2 min**	**vs. Na^+, Mg^{2+}, Ca^{2+}, Ni^{2+}, Zn^{2+}, Cu^{2+}**	**recyclable**	**This work**
Ni^{2+}	KMS-2	151	5 min	vs. alkali and alkaline earth cations	Not reusable	J. L. Mertz, Z. H. Fard, C. D. Malliakas, M. J. Manos and M. G. Kanatzidis, *Chem. Mater.*, 2013, **25**, 2116–2127
Ni^{2+}	S_x -LDH	106	-	not	Not reusable	S. Ma, Q. Chen, H. Li, P. Wang, S. M. Islam, Q. Gu, X. Yang and M. G. Kanatzidis, *J. Mater. Chem. A*, 2014, **2**, 10280–10289
Ni^{2+}	**Ca-MOF**	**84**	**5 min**	**vs. Na^+, Mg^{2+}, Ca^{2+}**	**recyclable**	**This work**
Zn^{2+}	S_x -LDH	106	-	vs. Ni^{2+}, Co^{2+}	Not reusable	S. Ma, Q. Chen, H. Li, P. Wang, S. M. Islam, Q. Gu, X. Yang

						and M. G. Kanatzidis, *J. Mater. Chem. A*, 2014, **2**, 10280–10289
Zn^{2+}	KMS-1	140	50 min	vs. Na^{+}, Mg^{2+}, Ca^{2+}	Not reusable	J. Li, L. Xu, M. Fu, Y. Wang and H. Xiao, ***Inorg. Chem. Front.***, 2018, **5**, 403-412
Zn^{2+}	**Ca-MOF**	**81**	**5 min**	**vs. Na^{+}, Mg^{2+}, Ca^{2+}**	**recyclable**	**This work**

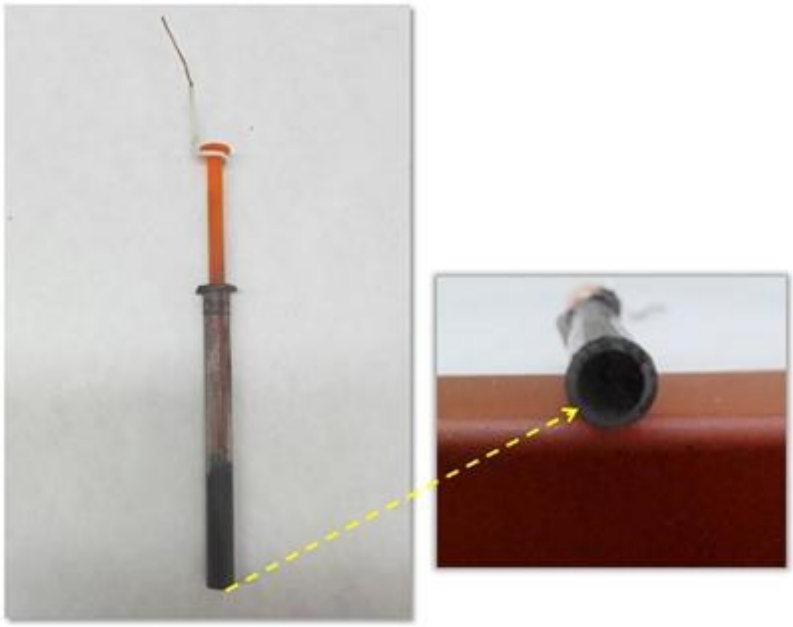

Fig. S1. Photographs of a used graphite paste electrode modified with **Ca-MOF** and of working electrode surface.

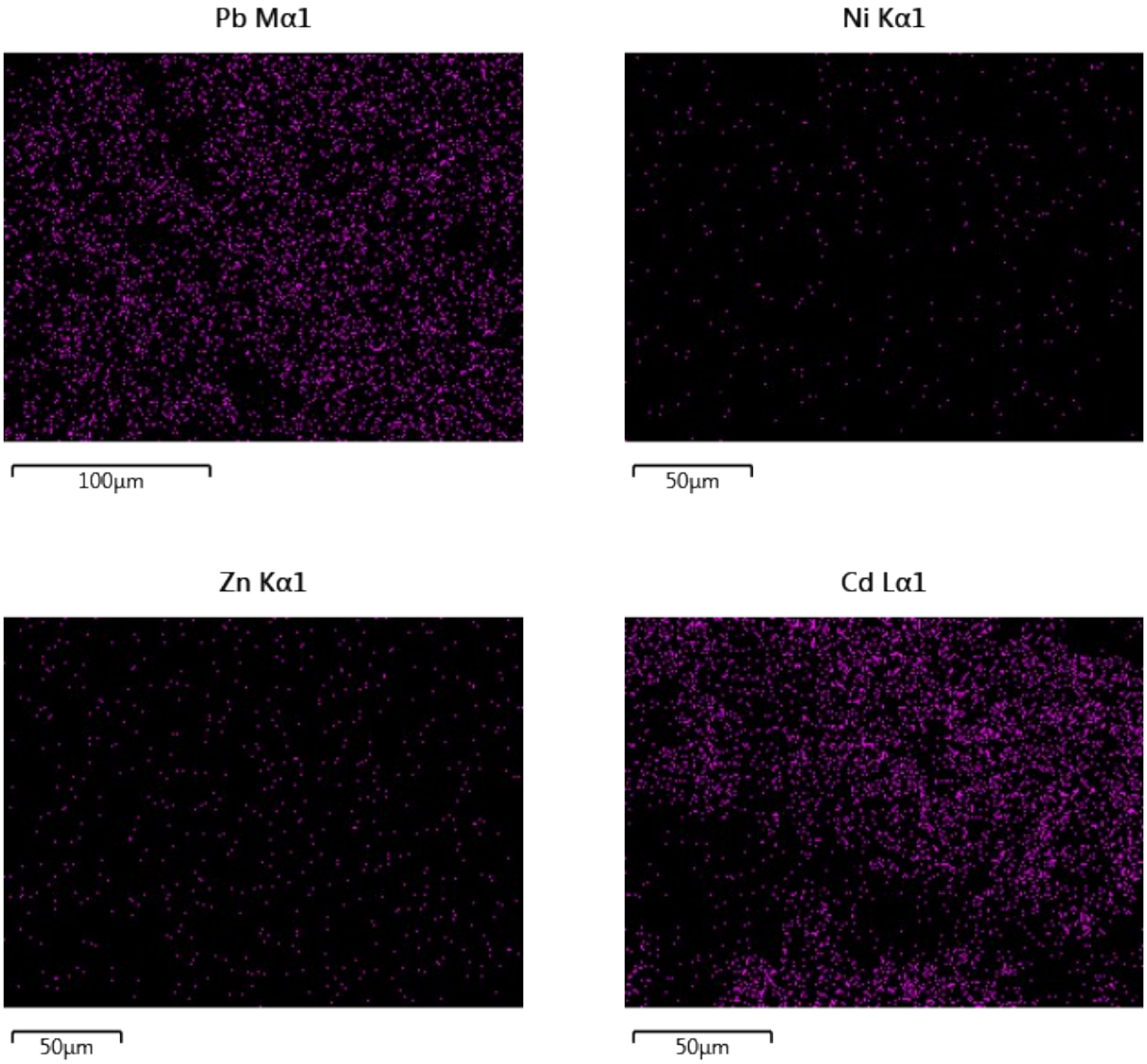

Fig. S2. EDS mapping of M^{2+} (M^{2+} = Pb^{2+}, Cd^{2+}, Ni^{2+}, Zn^{2+}) exchanged **Ca-MOF**. A typical ion-exchange experiment of **Ca-MOF** with M^{2+} (M^{2+} = Pb^{2+}, Cd^{2+}, Ni^{2+}, Zn^{2+}) is the following: In a solution of M^{2+} (0.36 mmol) in water (10 mL, pH was not adjusted), compound **Ca-MOF** (50 mg, 0.06 mmol,) was added as a solid. The mixture was kept under sonication and magnetic stirring for 1 h. Then, the solids were isolated by filtration, washed several times with water (5 × 10 mL) and acetone (1 × 5 mL) and dried in in a desiccator over silica gel overnight.

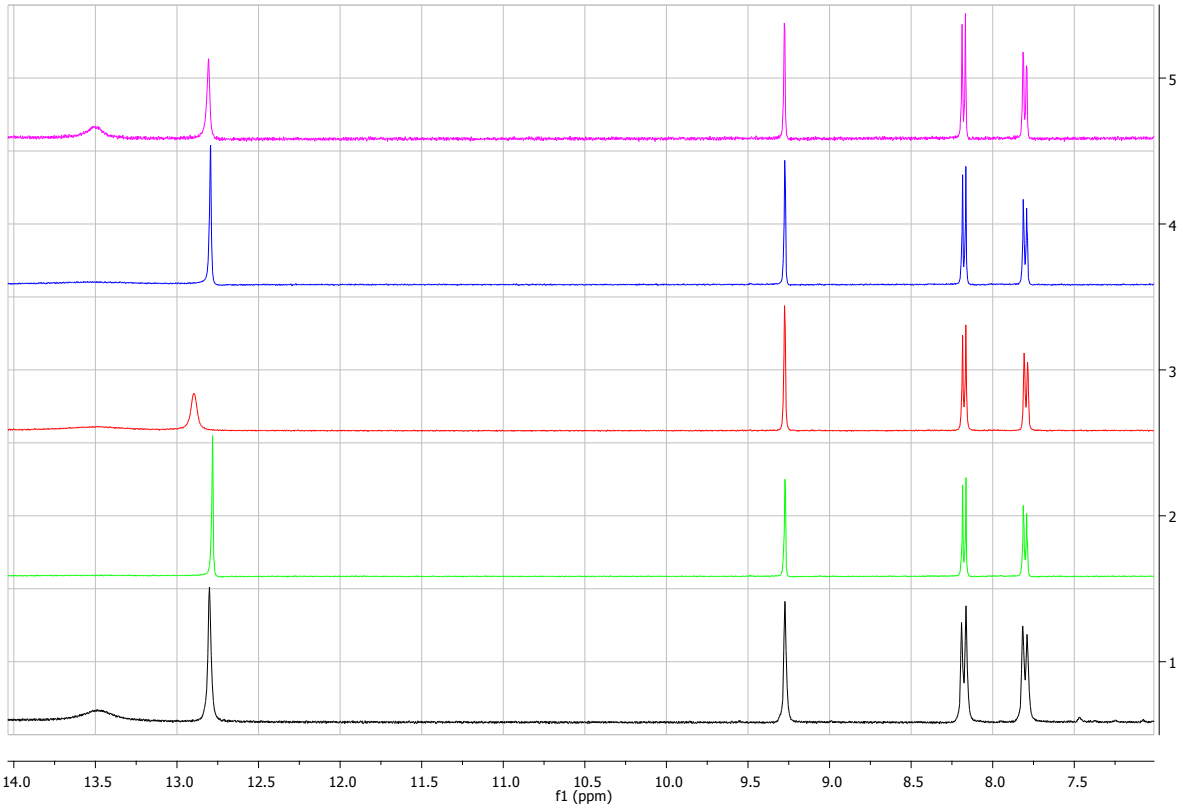

Fig. S3. The ^{1}H-NMR spectra in DMSO-d_6 of the as synthesized H_6L (bottom, black line), of H_6L recycled by treating the **Pb-MOF** (green line), **Ni-MOF** (red line), **Zn-MOF** (blue line) and **Cd-MOF** (magenta line) with HCl.

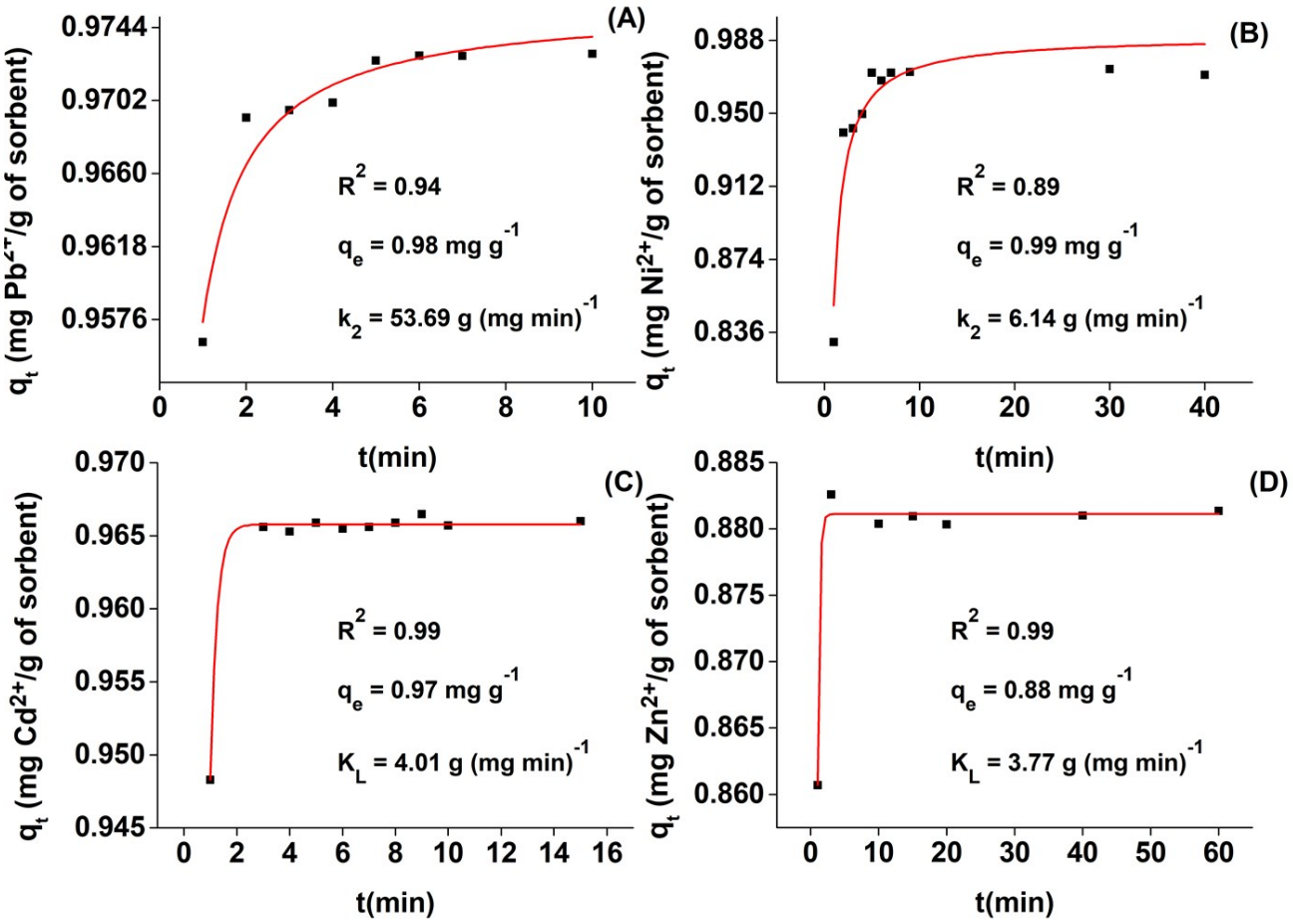

Fig. S4. Fitting of the kinetics data with the Ho-Mckay's second-order equation for the sorption of Pb^{2+} (A) and Ni^{2+} (B) by the **Ca-MOF**. Fitting of the kinetics data with the Lagergren's first-order equation for the sorption of Cd^{2+} (C) and Zn^{2+} (D) by the **Ca-MOF**.

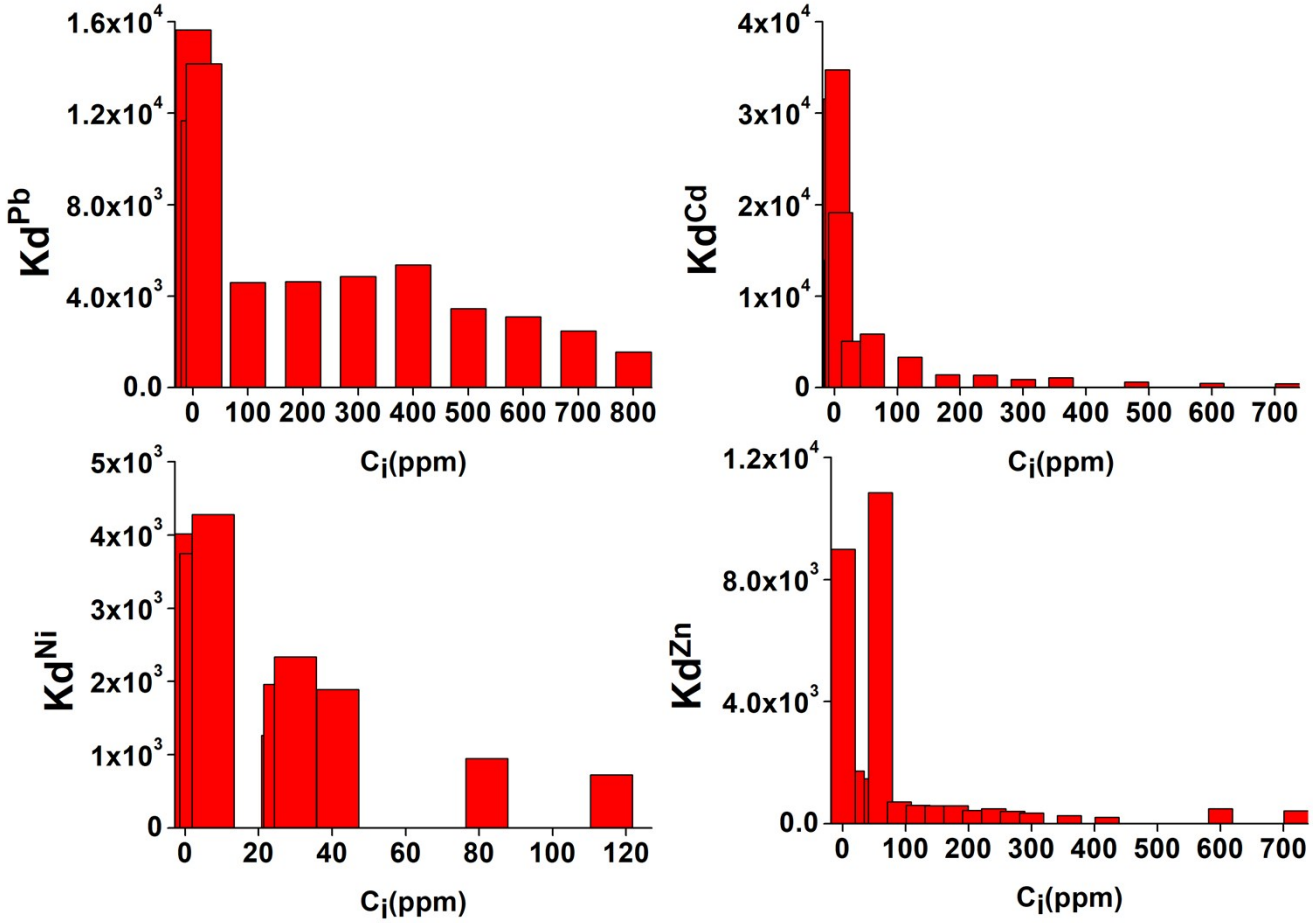

Fig. S5. The affinity of the **Ca-MOF** for Pb^{2+} (A), Ni^{2+} (B), Cd^{2+} (C) and Zn^{2+} (D) expressed in terms of the distribution coefficient K_d vs the initial concentration (C_i) of the metal ions.

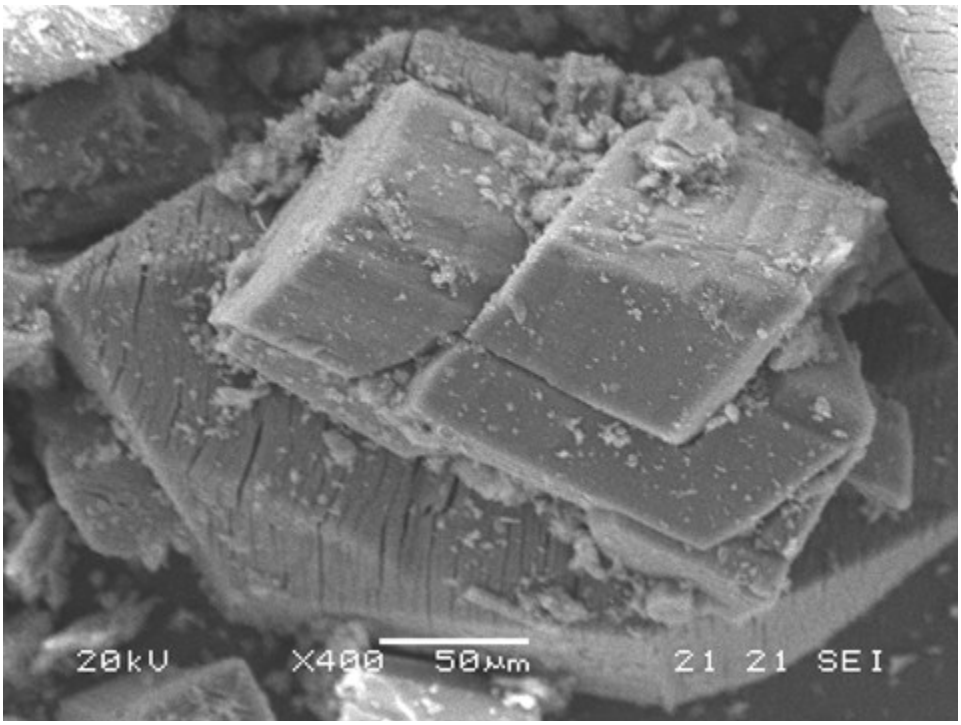

Fig. S6. SEM image of representative crystals of **Ca-MOF**.

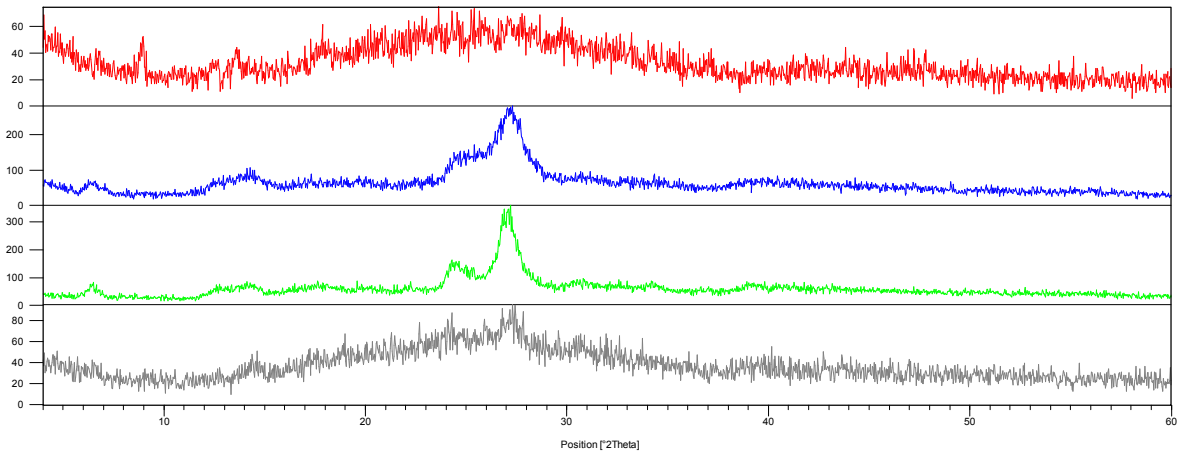

Fig. S7. Experimental powder X-ray diffraction patterns of **Pb-MOF** (red line), **Ni-MOF** (blue line), **Zn-MOF** (green line) and **Cd-MOF** (grey line).

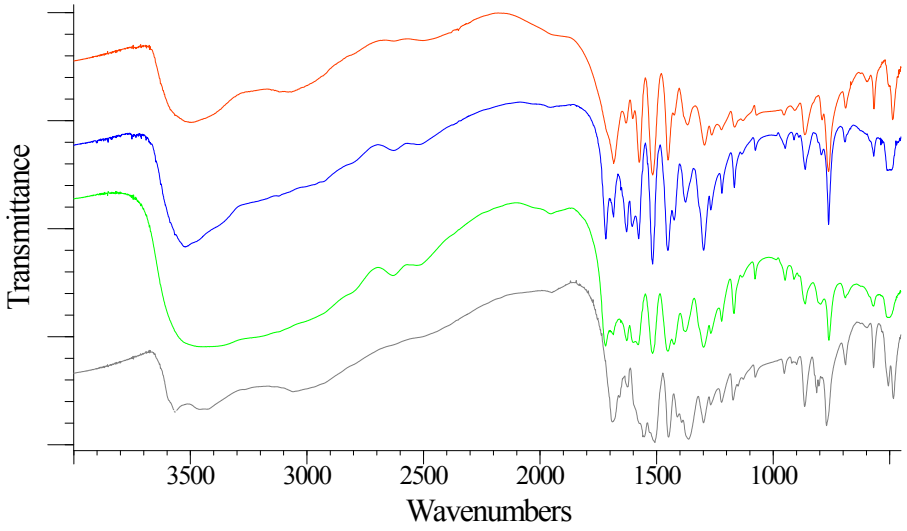

Fig. S8. The IR spectra (KBr pellets) of **Pb-MOF** (red line), **Ni-MOF** (blue line), **Zn-MOF** (green line) and **Cd-MOF** (grey line).

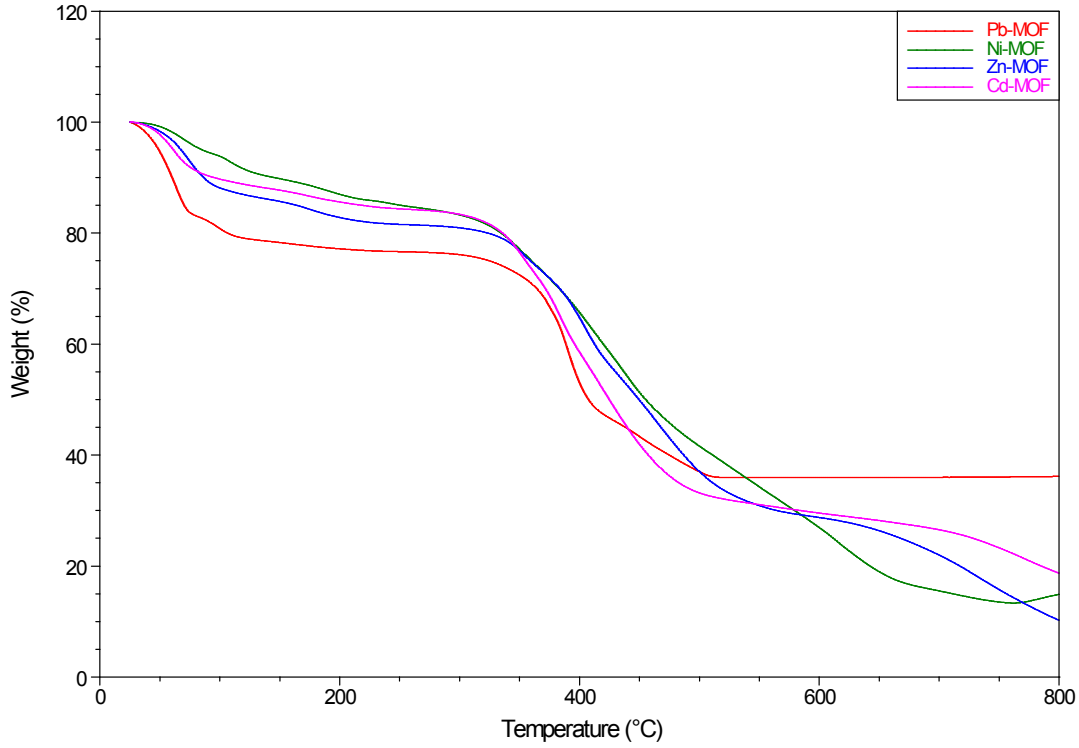

Fig. S9. TGA curves of **Pb-MOF** (red line), **Ni-MOF** (blue line), **Zn-MOF** (green line) and **Cd-MOF** (grey line).

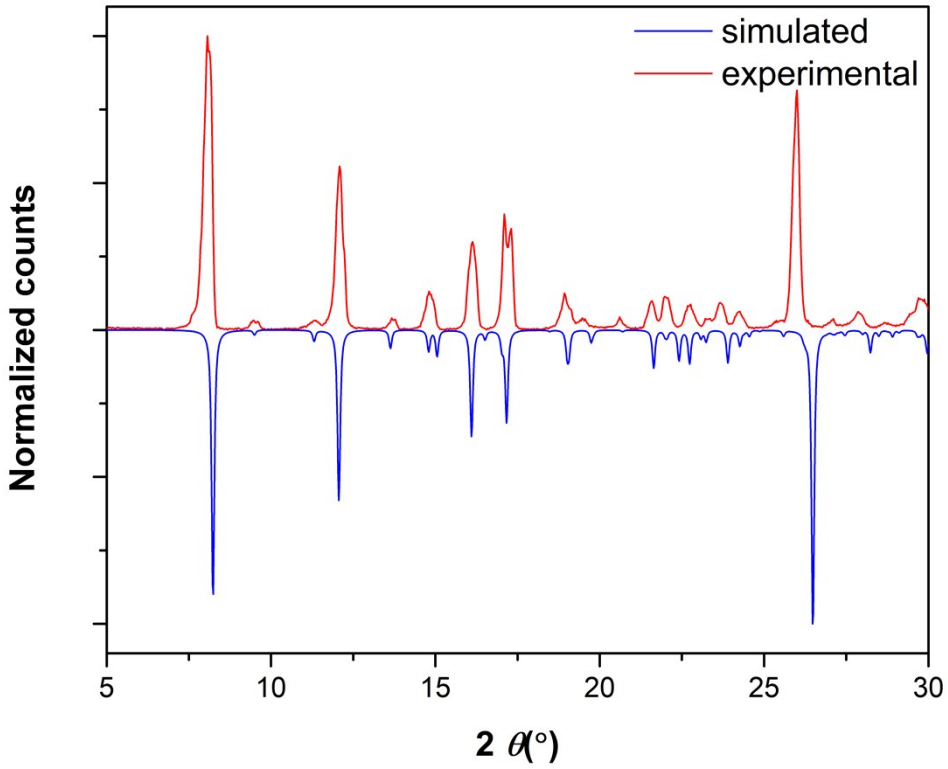

Fig. S10. Experimental (red line) and simulated (blue line) powder X-ray diffraction patterns (pxrds) of $[Ni(H_4L)(H_2O)_4]\cdot 2DMF$ (**1**).

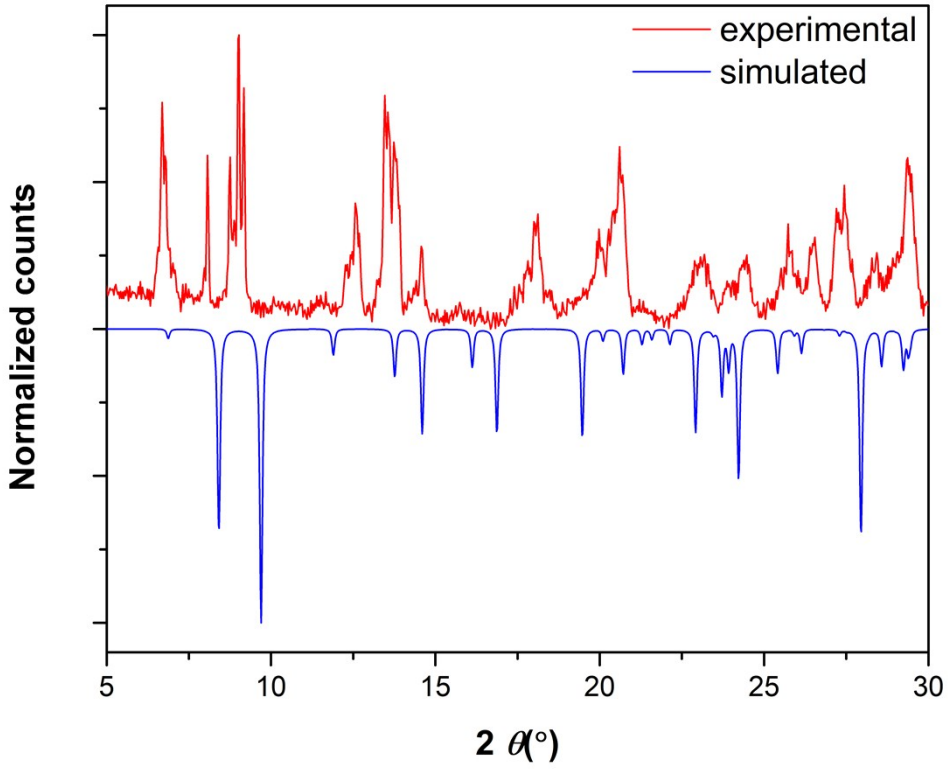

Fig. S11. Experimental (red line) and simulated (blue line) powder X-ray diffraction patterns (pxrds) of $[Pb_2(H_2L)]\cdot 2H_2O$ (**2**).

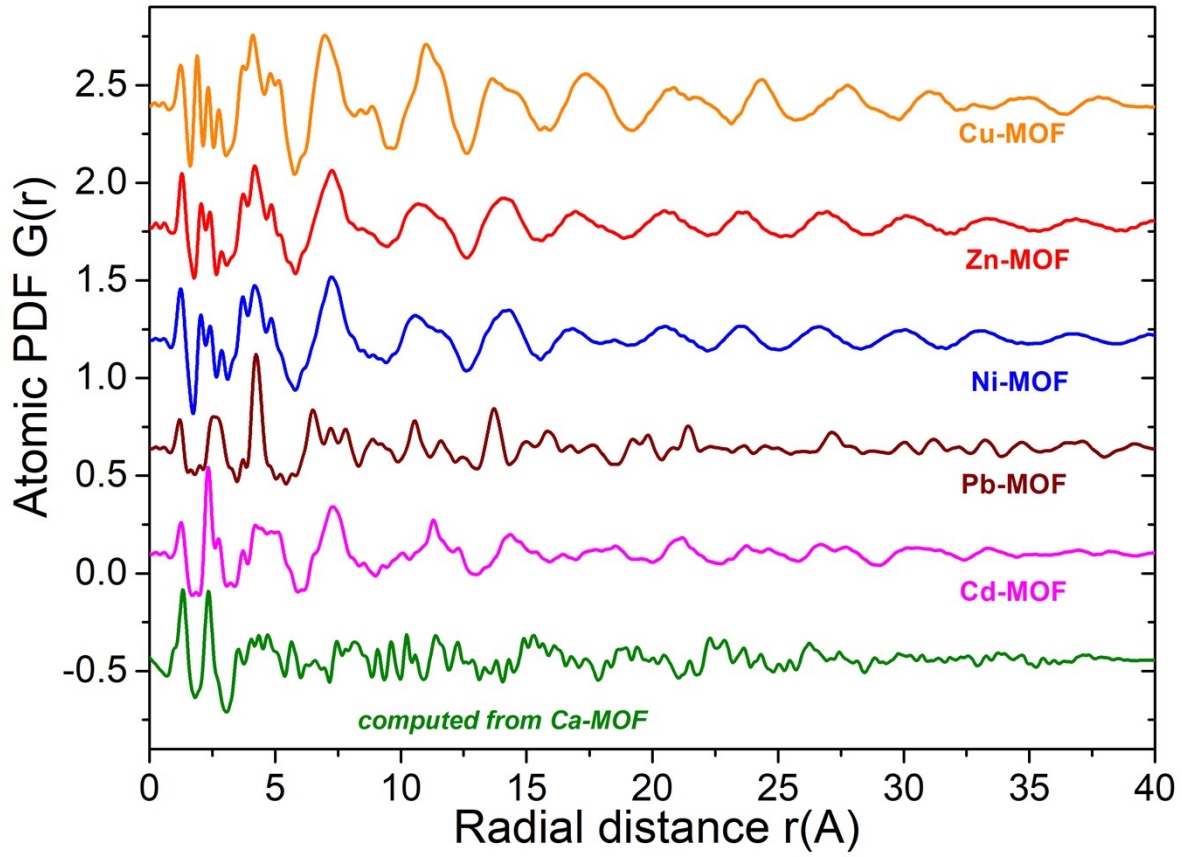

Fig. S12. Experimental atomic PDFs for **Cu-MOF**, **Zn-MOF**, **Ni-MOF**, **Pb-MOF** and **Cd-MOF**. Computed PDF for **Ca-MOF** is also shown.

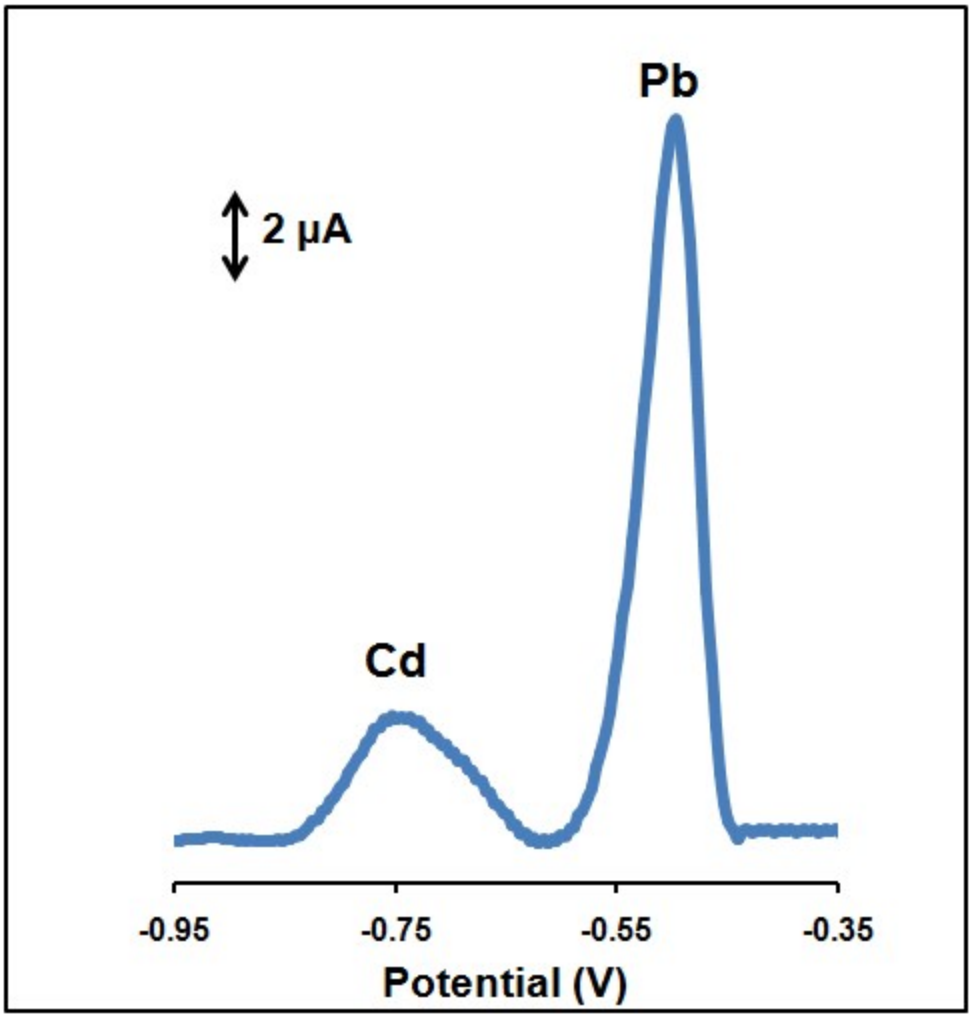

Fig. S13. SWASV voltammogram of 10 µg L^{-1} Cd(II) and 10 µg L^{-1} Pb(II) in acetate buffer 0.1 mol L^{-1}.

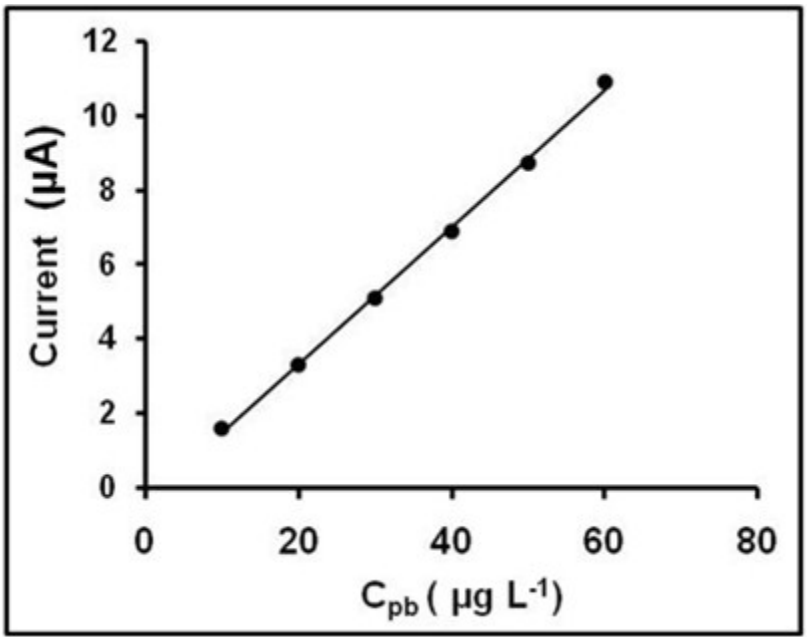

Fig. S14. Calibration plot of Pb(II) determination in the range 10-60 µg L^{-1} (step 10 µg L^{-1}) in acetate buffer 0.1 mol L^{-1} (pH 4.5) obtained with the **Ca-MOF**/GPE by differential pulse ASV.